Copper inverse-9-metallacrown-3 compounds interacting with DNA†

Tereza Afrati,[a] Anastasia A. Pantazaki,[c] Catherine Dendrinou-Samara,[a] Catherine Raptopoulou,[b] Aris Terzis[b] and Dimitris P. Kessissoglou*[a]

Received 14th July 2009, Accepted 29th September 2009
First published as an Advance Article on the web 4th November 2009
DOI: 10.1039/b914112j

Interaction of phenyl 2-pyridyl ketoxime (PhPyCNO)/X^- "blends" (X^- = OH^-, Cl^-, ClO_4^-, 2,4-D) (2,4-DH = 2,4-dichlorophenoxyacetic acid) with copper perchlorate has yielded trinuclear clusters that have been characterized as inverse-9-metallacrown-3, accommodating one or two anions. The structure of the complex $[Cu_3(PhPyCNO)_3(\mu_3\text{-}OH)(2,4\text{-}D)_2]\cdot 1.25CH_3OH\cdot 0.25CH_3CN$ (**1**) has been determined by single-crystal X-ray crystallography. Spectroscopic studies of the interaction of copper inverse {(OH)[9-$MC_{CuN(PhPyCNO)}$-3]} metallacrowns with DNA showed that these compounds bind to dsDNA by intercalative mode with an additional covalent {(OH)[9-$MC_{Cu(PhPyCNO)}$-3]}–DNA interaction leading to hydrolytic cleavage of DNA that may be assigned to the presence of the hydroxyl group in the inverse metallacrown ring. The binding strength of $[Cu_3(PhPyCNO)_3(\mu_3\text{-}OH)(2,4\text{-}D)_2]$ (**1**) complex for CT-DNA was determined to be 0.56×10^5 M^{-1}. All the complexes exhibited the ability to displace the DNA-bound EthBr. DNA electrophoretic mobility experiments showed that all complexes, at low cluster concentration, are capable of binding to pDNA and linear DNA. At higher cluster concentration and in the absence of any reducing agent they showed marked chemical nuclease activity.

Introduction

Inorganic polynuclear systems have drawn the attention of coordination chemists in the last two decades.[1,2] Metallacrowns (MC),[3] are usually formed with transition metal ions exhibiting selective recognition of cations and anions and the complexes can display intramolecular magnetic exchange interactions.[4–11] For 9-MC-3 metallacrowns, two structural motifs have been reported; regular and inverse. For the regular motif, the metallacrown ring is formed by repeating the [–O–N–M–] pattern with the oxygen atoms oriented towards the center of the cavity. For the inverse motif, the repeating pattern [–O–N–M–] remains the same, while the metal atoms are oriented towards the center of the cavity. The regular metallacrowns bind cations in a central cavity while the inverse metallacrowns can bind anions.

The majority of the inverse metallacrowns reported have been prepared with di-2-pyridyl-ketoxime (Hpko) or phenyl-pyridyl-ketoxime (PhPyCNO) as constructing ligands. PhPyCNO is a bifunctional ligand that can bind metals in five or six membered chelate rings showing a variety of coordination modes (Scheme 1). The interest in the synthesis of polynuclear, especially trinuclear, copper complexes and for the study of their physical and chemical properties stems from the recent knowledge that a trinuclear copper(II) center may be the functional unit in a number of blue oxidases.[12–15] It is also known that metal complexes may interact with DNA either covalently or non-covalently. In covalent binding the labile part of the complexes is replaced by a nitrogen base of DNA such as guanine N7 *e.g. cis*-platin.

On the other hand, non-covalent DNA interactions include intercalative, electrostatic and groove binding of cationic metal complexes along the outside of the DNA helix, the major or minor groove. Intercalation involves the partial insertion of aromatic heterocyclic rings between the DNA base pairs.[16,17] While many research efforts have been dedicated to the rational design and elaboration of biomimetics systems based on the interaction of

[a]*Department of General and Inorganic Chemistry, Aristotle University of Thessaloniki, Thessaloniki, 54124, Greece*
[b]*NCSR "Demokritos", Institute of Materials Science, 15310, Aghia Paraskevi Attikis, Greece*
[c]*Laboratory of Biochemistry, Department of Chemistry, Aristotle University of Thessaloniki, Thessaloniki, 54124, Greece*

† Electronic supplementary information (ESI) available: Figure S1. Electronic absorption spectra in the UV region of complexes **2**, **3** and **4** in the absence and presence of increasing amounts of CT-DNA; Figure S2. Electronic absorption spectra in the Vis region of complexes **2**, **3** and **4** in the absence and presence of increasing amounts of CT-DNA; Table S1. Absorption spectroscopic properties of DNA binding to the copper(II) complexes **1**, **2**, **3** and **4**. CCDC reference number 724337. For ESI and crystallographic data in CIF or other electronic format see DOI: 10.1039/b914112j

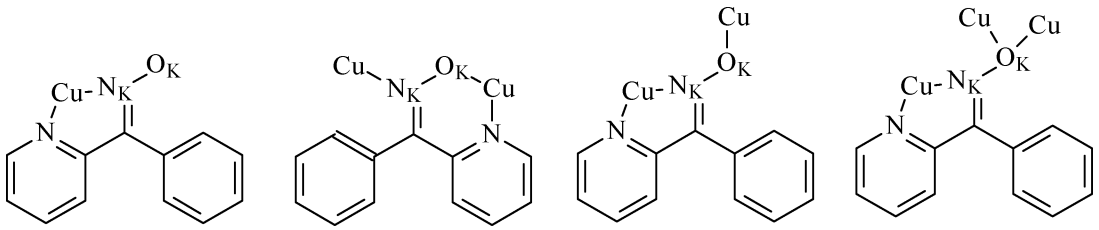

Scheme 1 The coordination binding modes of the PhPyCNO ligands observed in copper structures.

nucleobases and their derivatives with a wide range of metal ions, studies of polynuclear metal compounds are quite limited.[18]

Transition metal complexes also, stand out as candidates for artificial nucleases due to their diversity in structure and reactivity.[19–21] The biologically accessible oxidative/reductive potential made copper complexes a class of the most frequently studied metallonucleases. The $[Cu(phen)_2]^{2+}$ (phen = 1,10-phenanthroline) was the first Cu^{2+} complex displaying high efficiency for oxidative cleavage of DNA.[22,23] Currently polynuclear copper complexes are attracting much attention as artificial nucleases, since polynuclear metal centers are often found in natural nucleases and the metal centers may demonstrate synergistic effects in O_2 activation and DNA recognition.[24–36]

In a previous report, we have examined the magnetic, spectroscopic and structural features of a series of copper inverse {(OH)[9-$MC_{CuN(PhPyCNO)}$-3]} metallacrowns.[9–11] In addition, we have reported[37,38] studies on the effect of polynuclear metal complexes on the integrity and electrophoretic mobility of nucleic acids. Antifungal and antibacterial properties of a range of metal complexes have been evaluated against several pathogenic fungi and bacteria.[39–42]

In this article we report the synthesis and crystal structure of $[Cu_3(PhPyCNO)_3(\mu_3\text{-}OH)(2,4\text{-}D)_2]$ (**1**) (2,4-DH = 2,4-dichlorophenoxyacetic acid) and the study of interaction of inverse metallacrowns, $[Cu_3(PhPyCNO)_3(\mu_3\text{-}OH)(2,4,5\text{-}T)_2]$, (2,4,5-TH = 2,4,5-trichlorophenoxyacetic acid) (**2**),[11] $[Cu_3(PhPyCNO)_3(\mu_3\text{-}OCH_3)(Cl)(ClO_4)]$ (**3**)[10] and $[Cu_3(PhPyCNO)_3(\mu_3\text{-}OH)(CH_3OH)_2(ClO_4)_2]$ (**4**)[10] with DNA in an attempt to explore their potential biological activity with particular focus on their DNA binding mode or the ability of these clusters to function as DNA intercalators. Furthermore, DNA binding properties of the complexes with calf thymus DNA by spectroscopic titration were also investigated. Competitive binding studies with ethidium bromide, which is the most widely used intercalative agent and fluorescence probe for DNA structure, has been employed in the examination of the interaction of the copper inverse metallacrown clusters with DNA to investigate a potential intercalative binding mode. The nuclease activity of the complexes is also studied.

Results and discussion

The complexes $[Cu_3(PhPyCNO)_3(\mu_3\text{-}OH)(2,4,5\text{-}T)_2]$, (2,4,5-TH = 2,4,5-trichlorophenoxyacetic acid) (**2**),[11] $[Cu_3(PhPyCNO)_3(\mu_3\text{-}OCH_3)(Cl)(ClO_4)]$ (**3**)[10] and $[Cu_3(PhPyCNO)_3(\mu_3\text{-}OH)(CH_3OH)_2(ClO_4)_2]$ (**4**)[10] have been reported elsewhere. All the compounds, structurally characterized, form an inverse-9-metallacrown-3 core accommodating one or two anions and showing similar geometrical features.

The preparation of complex **1** can be achieved by the reaction of a mixture of $CuCl_2$ with $PhPyCNO^-$ in the presence of alkanoato sodium salts in MeOH solution at room temperature [eqn (1)].

$$3CuCl_2 + 3PhPyCNOH + 6NaOH + 2Cl_2C_6H_3OCH_2COOH \xrightarrow{MeOH} [Cu_3(PhPyCNO)_3(\mu_3\text{-}OH)(Cl_2C_6H_3OCH_2COO)_2] + 6NaCl + 5H_2O \quad (1)$$

All the compounds are dark green in colour and are soluble in DMF and DMSO, with **1** and **2** being non-electrolytes, **3** being a 1 : 1 electrolyte and **4**, a 1 : 2 electrolyte in these solvents. The IR spectrum of **1** exhibits characteristic bands due to the ligand $PhPyCNO^-$ [$\nu(C{=}N)_{pyridyl}$: 1595(s) and ν(N–O): 1460(*vs*)],[8–10] while the tentative assignments of the IR bands, the asymmetric $\nu_{asym}(CO_2)$ and the symmetric $\nu_{sym}(CO_2)$ stretching vibrations as well as the difference $\Delta = \nu_{asym}(CO_2) - \nu_{sym}(CO_2)$, useful characteristics for determining the coordination mode of carboxylato ligands, for the compound **1** are the following: a doublet strong band at 1605 cm^{-1} and 1580 cm^{-1} attributed to the $\nu_{asym}(CO_2)$ and a doublet strong band at 1405 and 1360 cm^{-1} attributed to the $\nu_{sym}(CO_2)$ stretching vibrations. The calculated Δ values suggest more than one coordination mode of the carboxylato ligands. Based on the crystal structure of **1** the values of Δ = 200 and 220 cm^{-1} may be excluded while Δ values of 175 and 245 cm^{-1} suggesting a bidentate bridging and a unidentate coordination mode respectively seem to be more realistic.[11]

Description of the structure of $[Cu_3(PhPyCNO)_3(\mu_3\text{-}OH)(2,4\text{-}D)_2]\cdot 1.25CH_3OH\cdot 0.25CH_3CN$ (1)

Selected bond distances and angles for complex **1** are listed in Table 1. The structure consists of a triangular unit, $[Cu_3(PhPyCNO)_3(\mu_3\text{-}OH)(2,4\text{-}D)_2]$. (Fig. 1). Complex **1** crystallizes in the triclinic space group $P\bar{1}$ with two crystallographically independent triangular units (molecules **1A** and **1B** respectively), 2.5 CH_3OH and 0.5 CH_3CN solvate molecules per asymmetric unit. The geometrical features of **1A** and **1B** are similar and only those of **1A**, given in Table 1, will be discussed.

The geometry of each copper(II) ion in the trimeric unit is best described as a distorted square-based pyramid with a NNOOO coordination environment. The trimeric unit is created by the oximato nitrogen atoms of a $PhPyCNO^-$ ligand and the oxime oxygen atom of the adjacent $PhPyCNO^-$ ligand, while a μ_3-OH^- completes the square-planar base of the three metal atoms

Table 1 Selected bond distances and angles of **1A**

Bond distances (Å)			
Cu1–OX1	1.958(6)	Cu2–N11	1.992(7)
Cu1–O11	1.941(6)	Cu2–O41	2.304(6)
Cu1–N2	1.974(7)	Cu3–OX1	1.922(6)
Cu1–N1	1.989(7)	Cu3–O1	1.942(6)
Cu1–O31	2.211(6)	Cu3–N21	1.972(7)
Cu2–O21	1.923(6)	Cu3–N22	1.981(7)
Cu2–OX1	1.943(6)	Cu3–O32	2.310(7)
Cu2–N12	1.969(7)		
Angles (°)			
O11–Cu1–N2	170.4(3)	O21–Cu2–N11	92.2(3)
O11–Cu1–OX1	92.9(2)	N12–Cu2–N11	80.8(3)
N2–Cu1–OX1	89.5(3)	O21–Cu2–N12	158.1(3)
N1–Cu1–OX1	166.7(3)	OX1–Cu3–N21	162.8(3)
O31–Cu1–OX1	89.9(2)	O1–Cu3–N22	176.7(3)
O31–Cu1–N1	100.3(3)	OX1–Cu3–O32	100.8(3)
O11–Cu1–N1	95.7(3)	O1–Cu3–O32	91.0(3)
N2–Cu1–N1	80.4(3)	N21–Cu3–O32	93.7(3)
O11–Cu1–O31	89.8(2)	OX1–Cu3–O1	92.9(3)
N2–Cu1–O31	99.5(3)	O1–Cu3–N21	96.1(3)
N12–Cu2–O41	94.5(3)	OX1–Cu3–N22	89.9(3)
O21–Cu2–OX1	94.7(3)	N21–Cu3–N22	80.8(3)
OX1–Cu2–N12	90.2(3)	N22–Cu3–O32	90.2(3)
OX1–Cu2–N11	170.1(3)	Cu3–OX1–Cu2	113.9(3)
OX1–Cu2–O41	92.1(2)	Cu3–OX1–Cu1	106.5(3)
N11–Cu2–O41	92.8(3)	Cu2–OX1–Cu1	109.8(3)
O21–Cu2–O41	106.7(2)		

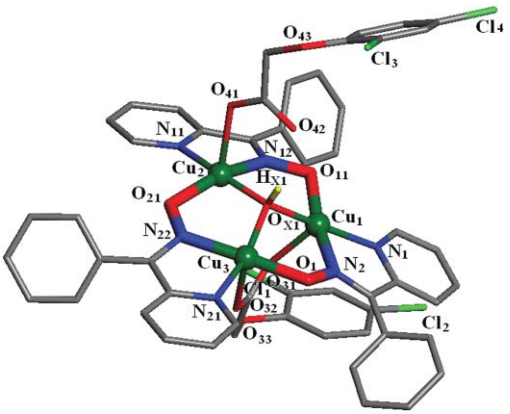

Fig. 1 X-Ray crystal structure of $[Cu_3(PhPyCNO)_3(\mu_3\text{-}OH)\text{-}(2,4\text{-}D)_2]\cdot 1.25CH_3OH\cdot 0.25CH_3CN$ (**1**), with heteroatoms labeled.

with bond distances of Cu(1)–OX(1) = 1.958(6), Cu(2)–OX(1) = 1.943(6) and Cu(3)–OX(1) = 1.922(6) Å. Two alkanoato ligands are bound to trimeric units on the opposite sides in bidentate and unidentate mode. The bidentate alkanoato ligand bridges Cu1 and Cu3 with Cu1–O31 = 2.211(6) Å and Cu3–O32 = 2.310(7) Å distances while the oxygen of the unidentate ligand occupies the apex position of the Jahn–Teller elongated square-base pyramid to a Cu2–O41 = 2.304(6) distance creating a hydrogen bond with the hydroxyl group accommodated by the inverse metallacrown ring [O42···HOX1 = 1.936 Å, OX1···O42 = 2.584 Å, OX1–HOX1···O42 = 147.5°]. The four atoms that define each of the three basal planes around the Cu(II) ions deviate slightly from planarity with torsion angles of 179.45° and 179.46° for Cu(1), 164.41° and 164.84° for Cu(2) and 164.22° and 166.62° for Cu(3) while the copper atoms lie on the square basal planes with the sum of the angles around each copper atom = 358.57° for Cu(1) 357.95° for Cu(2) and 359.63° for Cu(3). The Cu_3 can be considered as an equilateral triangle with distances of 3.109(2) Å, (Cu(1)···Cu(3)), 3.239(5) Å (Cu(2)···Cu(3)), and 3.192(5) Å (Cu(1)···Cu(2)).

The *inverse*-$9MC_{Cu(II)(PhPyCNO)}$-3 is almost planar with torsion angles varying from 170° to 179°. The oxygen atom of the hydroxy ligand, trapped in the metallacrown ring lies out of the plane defined by the copper atoms at a distance of 0.63 Å.

Titration spectroscopic studies of copper(II) complexes with DNA

The integrity of the trinuclear unit in solution is a key consideration in interpretation of the data. Based on our previous reports[10,11] our data support this hypothesis. Furthermore, compound **1** is not an electrolyte in DMSO or DMF. We have also studied the interaction of $Cu(ClO_4)_2$ or $Cu_2(alkanoato)_4$ with DNA by spectroscopic titration in order to be sure that this interaction is not related to mononuclear or dinuclear species. To that extent, no isosbestic point was detected at 910 nm. In order to be clear that in the DMSO–buffer mixture the trinuclear species remain intact, we have also shown that the molecular conductance of the DMSO–buffer solution with and without compound **1** does not show noticeable differences.

Electronic absorption spectroscopy is universally employed to determine the binding of complexes with DNA. Complexes bound to DNA through intercalation or in an electrostatic manner usually result in hypochromism and red shift (bathochromism) due to the intercalative mode involving a strong stacking interaction between the aromatic chromophore and the base pairs of DNA. Hypochromism and hyperchromism are the spectral features of DNA concerning its double helix structure. Hypochromism means the DNA binding mode of the complex is intercalation or electrostatic effect,[43,44] which can stabilize the DNA duplex, and hyperchromism means the breakage of the secondary structure of DNA.[45,46]

The absorption spectra of the complexes $[Cu_3(PhPyCNO)_3(\mu_3\text{-}OH)(2,4\text{-}D)_2]$ (**1**), $[Cu_3(PhPyCNO)_3(\mu_3\text{-}OH)(2,4,5\text{-}T)_2]$, (2,4,5-TH = 2,4,5-trichlorophenoxyacetic acid) (**2**), $[Cu_3(PhPyCNO)_3\text{-}(\mu_3\text{-}OCH_3)(Cl)(ClO_4)]$ (**3**) and $[Cu_3(PhPyCNO)_3(\mu_3\text{-}OH)\text{-}(CH_3OH)_2(ClO_4)_2]$ (**4**) in the presence of calf thymus DNA show similar changes due to the structural similarities.

The electronic absorption spectra of **1** at 341 nm (Fig. 2) upon titration with calf thymus DNA for ratios R = [CT-DNA]/[complex]) = 0 to 1.980, show 40.51% absorbance hypochromism for the intraligand (IL) band and a red shift of about 4 nm. This strong hypochromism suggests an intercalative mode of binding that involves a stacking interaction between the complex and the base pairs of DNA. The presence of free aromatic rings in all complexes supports the hypothesis that an aromatic moiety overlaps with the stacking base pairs of DNA.

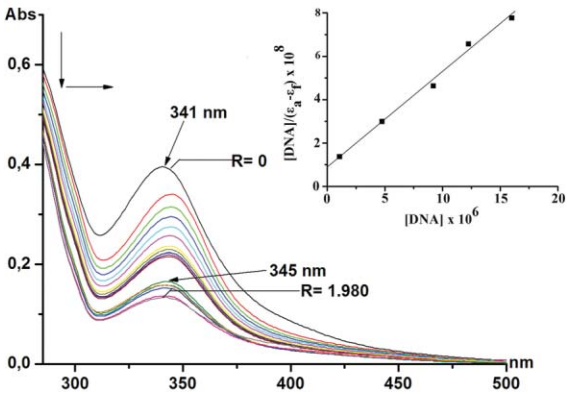

Fig. 2 Electronic absorption spectra in the UV region of $[Cu_3(PhPyCNO)_3(\mu_3\text{-}OH)(2,4\text{-}D)_2]$ (**1**), in the absence (R = 0) and in the presence of increasing amounts of CT-DNA. [complex] = 2.5×10^{-5} M, R = [CT-DNA]/[complex]. Arrows show the absorbance changes upon increasing CT-DNA concentration. Inset shows the typical plot of $[DNA]/(\varepsilon_a - \varepsilon_f)$ *versus* [CT-DNA].

The intense d–d absorption band of copper complexes in the Vis region is also used to monitor the interaction of DNA with the complexes. In Fig. 3 the electronic absorption spectra of **1** upon titration with calf thymus DNA is shown.

For ratios R = 0 to 1.980 gradual hypochromism for the d–d absorption band at 651 nm and a blue shift of about 9 nm are observed while a new band at 981 nm appears forming an isosbestic point at 912 nm. These spectral changes can be attributed to the interaction of inverse-{(OH)[9-$MC_{Cu(II)N(PhPyCNO)}$-3]}-DNA by an intercalative binding mode leading to hydrolytic cleavage of DNA that may be assigned to the presence of the hydroxyl group in the inverse metallacrown ring. It has been reported previously that $Cu(ClO_4)_2$ does not effect detectable cleavage of plasmid DNA, while trinuclear copper complexes have several exchangeable labile coordination sites so a hydrolytic mechanism could also operate by

Table 2 Absorption spectroscopic properties in the UV region of the copper(II) complexes **1**, **2**, **3** and **4** binding to DNA

Comp.	*R*	λ_{max}/nm	Change in absorbance	Red shift/nm	Blue shift/nm	Hypo. (%)	K_b/M^{-1}
1	0	341	Hypochromism	4	—	40.51	0.56×10^5
	1.980	345					
2	0	347	Hypochromism	—	6	52.08	1.96×10^5
	1.980	341					
3	0	348	Hypochromism	—	7	55.14	2.23×10^5
	1.980	341					
4	0	345	Hypochromism	—	3	54.25	2.06×10^5
	1.980	342					

R = [DNA]/[complex], concentration of copper solutions 2.5×10^{-5} M, Hypo. = Hypochromism.

Table 3 Absorption spectroscopic properties in the Vis region of the copper(II) complexes **1**, **2**, **3** and **4** binding to DNA

Comp.	*R*	λ_{max}/nm	Change in absorbance	Red shift/nm	Blue shift/nm	Hypo. (%)
1	0	651	Hypochromism	—	9	29.33
	1.980	642				
2	0	649	Hypochromism	—	10	40.20
	1.980	639				
3	0	642	Hypochromism	5	—	49.01
	1.980	647				
4	0	634	Hypochromism	5	—	47.55
	1.980	639				

R = [DNA]/[complex], concentration of copper solutions 5×10^{-4} M, Hypo. = Hypochromism.

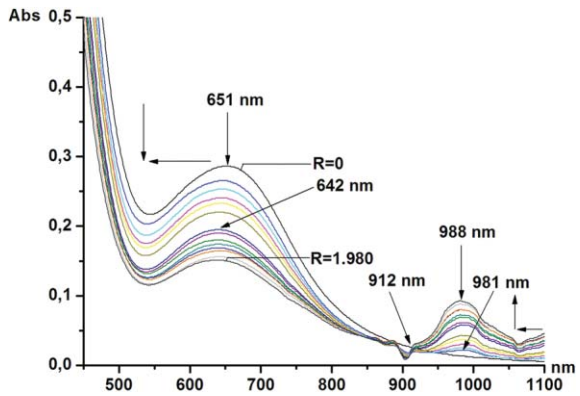

Fig. 3 Electronic absorption spectra in the Vis region of $[Cu_3(PhPyCNO)_3(\mu_3\text{-}OH)(2,4\text{-}D)_2]$ (**1**), in the absence ($R = 0$) and in the presence of increasing amounts of CT-DNA. [complex] = 5×10^{-4} M, R = [CT-DNA]/[complex]. Arrows show the absorbance changes upon increasing CT-DNA concentration.

the formation of a Cu(II)–OH hydroxyl group which might serve as a nucleophilic agent to attack DNA.[24] Catalytic hydrolysis of phosphodiesters was also observed with $[Cu(bipy)]^{2+}$ and the rate of hydrolysis increased with pH, supporting the participation of a Cu–OH in the hydrolytic mechanism.[47,48] Gel electrophoresis data (see below) also suggest that these complexes are capable of cleaving DNA by a discernible hydrolytic path. Therefore we might assign the new band at 981 nm to the formation of a $\{(OH)[9\text{-}MC_{Cu(II)N(PhPyCNO)}\text{-}3]\}$-{cleaved-DNA} chromophore with tetrahedral geometrical distortion around metal atoms.

We obtained the binding constants by monitoring the changes in absorbance (at 341 nm for complex **1**) with increasing concentrations of DNA, according to the equation:[49–52]

$$[DNA]/(\varepsilon_a - \varepsilon_f) = [DNA]/(\varepsilon_b - \varepsilon_f) + 1/K_b(\varepsilon_b - \varepsilon_f),$$

where [DNA] is the concentration of DNA in base pairs, and ε_a, ε_f and ε_b correspond to the ratio A_{abs}/[complex], the molar absorptivity for the free copper complex, and the molar absorptivity for the copper complex in the fully bound form, respectively. In a plot of $[DNA]/(\varepsilon_a - \varepsilon_f)$ *versus* [DNA], K_b is given by the ratio of the slope to the y intercept. For complexes **1**–**4** the K_b values 0.56×10^5, 1.96×10^5, 2.23×10^5 and 2.06×10^5 M^{-1} respectively are similar suggesting interaction with DNA in a similar manner. The absorption spectroscopic properties in the UV and Vis region of the copper(II) complexes **1**, **2**, **3** and **4** binding to DNA are given in Table 2 and Table 3, respectively.

According to the data (Fig. 2, 3, S1 and S2†), it seems that the spectral perturbation of **1** upon addition of DNA is similar to that of the other complexes, with the intraligand absorption band but exhibiting the lower hypochromism. This implies that the binding modes with DNA may be the same. The K_b values are lower than those observed for typical classical intercalators (ethidium–DNA, 1.4×10^6 M^{-1} in 25 mM Tris-HCl/40 mM NaCl buffer, pH = 7.6).[53]

In the UV region the intense DNA based ($\pi \rightarrow \pi^*$) absorption band may be also used to monitor the interaction of DNA with the complexes. In Fig. 4 the electronic absorption spectra upon addition of increasing amounts of complex **1** to 1.2×10^{-4} M CT-DNA, is shown.

Gradual hyperchromism of CT-DNA absorption at 260 nm with a blue shift of 4 nm is observed and the relationship between hyperchromism and copper(II) complex concentrations is linear at the molar ratio ranging from 0 to 0.02, suggesting the breakage of hydrogen bonds stabilizing the secondary structure of the DNA double helix, while the absorption band characteristic of the complex at 347 nm appeared at higher complex concentrations.

Table 4 Absorption spectroscopic properties of the copper(II) complexes **1**, **2**, **3** and **4** binding to guanine (Hyper. = Hyperchromism)

Complex	λ_{max}/nm	Blue shift/nm	Change in absorbance	Hyper. (%)	Isosbestic point/nm
1	651	17	Hyperchromism	11.81	512
2	649	10	Hyperchromism	10.33	512
3	642	5	Hyperchromism	9.40	498
4	634	1	Hyperchromism	11.84	505

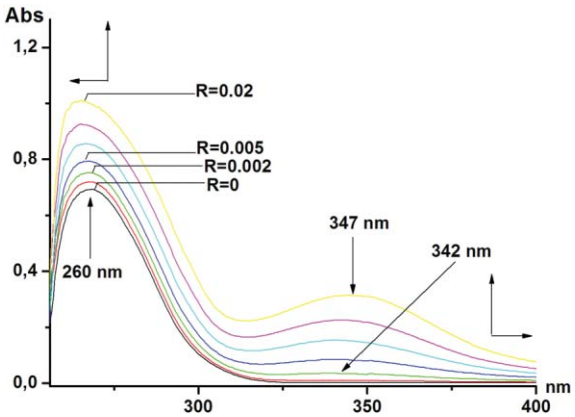

Fig. 4 Absorption spectra of 1.2×10^{-4} M CT-DNA in the absence ($R = 0$) and in the presence of increasing amounts of $[Cu_3(PhPyCNO)_3(\mu_3\text{-}OH)(2,4\text{-}D)_2]$ (**1**) from $R = 0$ to 0.02. Arrows show the absorbance changes upon increasing complex concentration. R = [complex]/[CT-DNA].

Similar behavior was observed for the other complexes, data not shown (Table S1†).

Spectroscopic studies of copper(II) complexes with DNA components

In order to gain support for the formation of a {(OH)[9-$MC_{Cu(II)N(PhPyCNO)}$-3]}–{cleaved-DNA} chromophore we have investigated the interaction of the complexes with DNA components like guanine, guanosine-5′-monophosphate (GMP) and adenosine-5′-monophosphate (AMP) using electronic absorption spectral techniques.

For all complexes the guanine causes significant blue shifts and hyperchromism accompanied by an isosbestic point at 512 nm (Table 4, Fig. 5) indicating possible binding of the complexes to the N7 nitrogen of guanine.

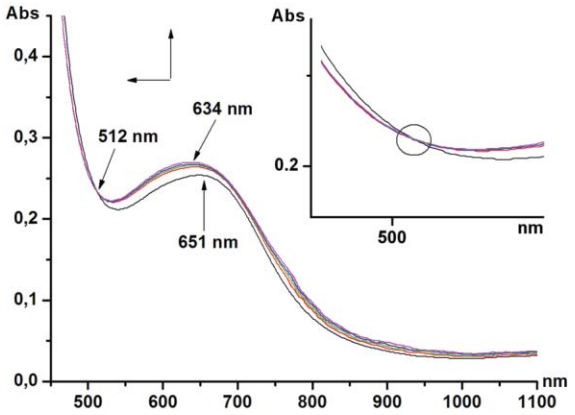

Fig. 5 Absorption spectra of 5×10^{-4} M $[Cu_3(PhPyCNO)_3(\mu_3\text{-}OH)(2,4\text{-}D)_2]$ (**1**) in the absence of ($R = 0$) and presence of increasing amounts of guanine. Arrows show the absorbance changes upon increasing guanine concentration. [guanine] = 6.98×10^{-5}, 7.14×10^{-5}, 7.32×10^{-5} and 7.50×10^{-5} M, respectively.

AMP and GMP cause significant hypochromism and blue shifts in the d–d band of the complexes accompanied by an isosbestic point at about 910 nm (Table 5, Fig. 6). The spectral changes were similar for all complexes and identical to those of the CT-DNA titration experiments. These spectroscopic variations, concerning the effectiveness order compared with those obtained from guanine may be assigned to the presence of the phosphate in

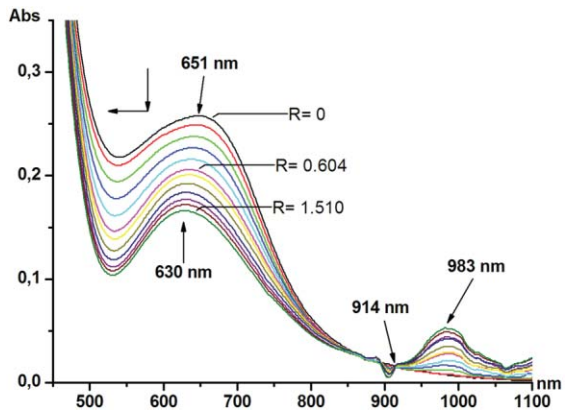

Fig. 6 Absorption spectra of 5×10^{-4} M $[Cu_3(PhPyCNO)_3(\mu_3\text{-}OH)(2,4\text{-}D)_2]$ (**1**) in the absence ($R = 0$) and presence of increasing amounts of AMP. Arrows show the absorbance changes upon increasing AMP concentration. R = [AMP]/[Complex].

Table 5 Absorption spectroscopic properties of the copper(II) complexes **1**, **2**, **3** and **4** binding to AMP and GMP (Hypo. = Hypochromism)

Complex	λ_{max}/nm	Change in absorbance	Blue shift/nm	Hypo. (%)	Isosbestic point/nm	K_b/M^{-1}
			AMP			
1	651	Hypochromism	21	42.58	914	4.49×10^3
2	649	Hypochromism	20	30.39	921	4.48×10^3
3	642	Hypochromism	13	16.20	907	4.18×10^3
4	634	Hypochromism	1	30.23	908	4.22×10^3
			GMP			
1	651	Hypochromism	17	12.54	927	2.87×10^3
2	649	Hypochromism	14	30.50	928	3.38×10^3
3	642	Hypochromism	11	13.18	917	3.19×10^3
4	634	Hypochromism	2	6.63	929	2.59×10^3

the GMP or AMP. Binding constants, K_b, of GMP or AMP to the complexes obtained by monitoring the changes of the d–d bands suggest similar binding strength.

Fluorescence spectroscopic studies

Ethidium bromide (EthBr) emits intense fluorescent light in the presence of DNA due to its strong intercalation between the adjacent DNA base pairs. It has been previously reported[54–57] that the enhanced fluorescence could be quenched by the addition of a complex capable of intercalating into the DNA base pairs replacing the bound EthBr (if it binds to DNA more strongly than EthBr) or by accepting the excited state electron from EthBr or breaking the secondary DNA structure. In fact, the extent of fluorescence quenching for EthBr bound to DNA can be used to determine the extent of binding between another molecule and DNA.[55,56] The study involves addition of the complexes to DNA pre-treated with EthBr and then measurement of the intensity of emission.

Thus, on the addition of each of the present metal complexes to CT-DNA pre-incubated with EthBr ([CT-DNA]/[EthBr] = 1) the DNA-induced EthBr emission decreased gradually, when the molar ratio of the complexes to CT-DNA (r = [complex]/[CT-DNA]) range from 0 to 0.737, as shown in Fig. 7. In similar cases two mechanisms have been proposed to account for the quenching of EthBr emission, the replacement of the molecular fluorophores and electron transfer. The non replacement-based quenching has been correlated with DNA-mediated electron transfer from the excited ethidium bromide to an acceptor (*e.g.*, cupric ion, Cu^{2+}).[58,59]

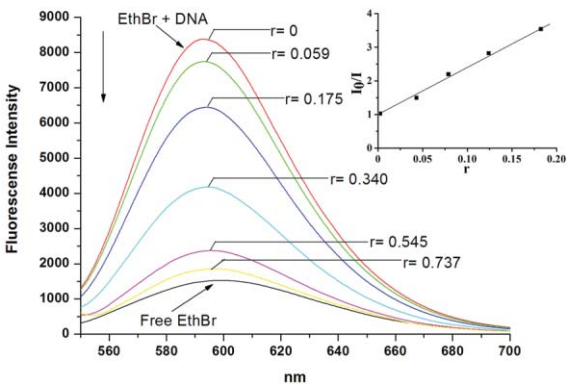

Fig. 7 Fluorescence spectra of EthBr binding to DNA in the absence (r = 0) and presence of increasing amounts of $[Cu_3(PhPyCNO)_3(\mu_3\text{-}OH)(2,4\text{-}D)_2]$ (**1**), λ_{ex}= 540 nm, [EthBr] = 1.6×10^{-4} M, [CT-DNA] = 1.6×10^{-4} M, r = 0–0.737. The inset is the Stern–Volmer quenching plot. r = [complex]/[CT-DNA]. Arrows show the intensity changes upon increasing complex concentration.

However it is notable that on further addition of the complex to the ratio 0.915 the fluorescence became almost the same as that of free EthBr (Fig. 8). This indicates that the DNA binding of the complexes to DNA lead to the release of intercalatively bound EthBr. On the addition of more complex (from r = 0.915 to r = 2.390), the fluorescence starts enhancing gradually again. In addition a shift of 10 nm at higher wavelengths and a shoulder at 658 nm is observed (Fig. 8).

All these results are indicative that the CT-DNA interacts with metallacrown complexes in two different modes. At low molar

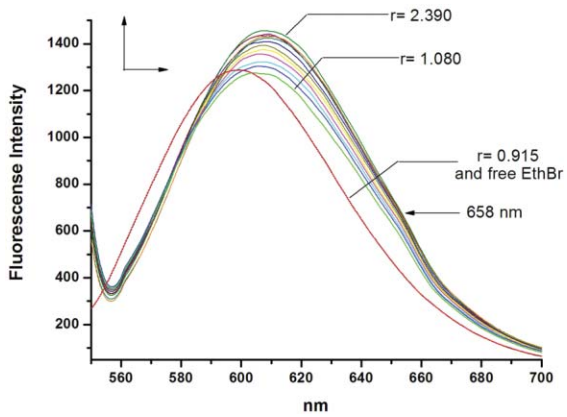

Fig. 8 Fluorescence spectra of EthBr binding to DNA in the absence (r = 0) and in the presence of increasing amounts of $[Cu_3(PhPyCNO)_3(\mu_3\text{-}OH)(2,4\text{-}D)_2]$ (**1**), λ_{ex} = 540 nm, [EthBr] = 1.6×10^{-4} M, [CT-DNA] = 1.6×10^{-4} M, r = 0.915–2.390, r = [complex]/[CT-DNA]. Arrows show the intensity changes upon increasing complex concentration. The dotted line represents the fluorescence intensity of free EthBr and the solid line at r = 0.915.

ratio (ranging from 0–0.737), the complex may replace the bound EthBr and break down the DNA secondary structure of the double helix quenching the fluorescence. At higher molar ratio (ranging from 0.915–2.390), the enhancement of fluorescence, as well as the presence of shift and the shoulder observed in the spectra might be attributed eventually to EthBr intercalation into the base pairs again and simultaneously to the formation of new DNA products. These results are consistent with those obtained from the titration spectroscopic studies of the copper(II) complexes with DNA. Similar behaviour has also been observed for the complex $[Cu_2Phen_2Cl_4]$.[54]

The quenching efficiency for each complex is evaluated by the Stern–Volmer constant K_{sp}, which varies with the experimental conditions:[56]

$$I_0/I = 1 + K_{sp}r,$$

where I_0 and I represent the fluorescence intensities in the presence of the complex, respectively, and r is the concentration ratio of the complex to DNA. K_{sq} is a linear Stern–Volmer quenching constant dependent on the ratio of the bound concentration of EthBr to the concentration of DNA (seen in Fig. 7). The K_{sq} value is obtained as the slope of I_0/I *versus* r linear plot. The K_{sq} values for the complexes **1**, **2**, **3** and **4** are 1.03, 1.19, 2.58 and 1.70, respectively. Such values of quenching constant suggest that the interaction of the complexes with DNA is strong.[55,60] The K_{sq} values are well consistent with the above absorption spectral results.

Cleavage of pDNA by {(OH)[9-MC$_{Cu(II)N(PhPyCNO)}$-3]} metallacrowns and concentration-dependence of the reaction

The DNA endonucleolytic cleavages caused by metal ions, have been of interest to researchers.[61] Transition metal-mediated radical production may result in an efficient DNA cleavage. It is known that DNA cleavage is reflected by relaxation of the supercoiled circular form of pET29c DNA resulting in nicked circular and/or linear forms. When electrophoresis is applied to circular plasmid DNA, the fastest migration will be observed for DNA of closed circular forms (Form I, supercoiled). If one strand is cleaved, the

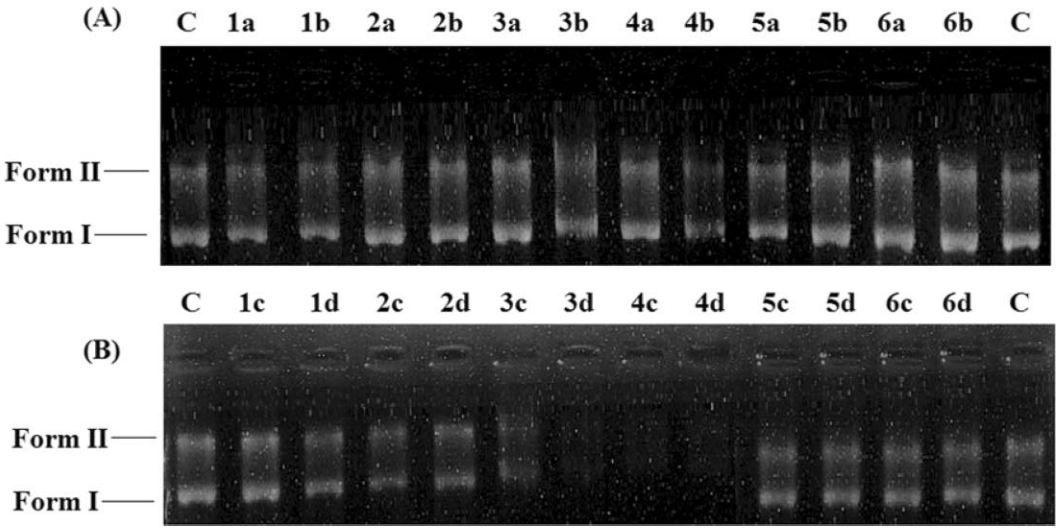

Fig. 9 Agarose (1%w/v) gel electrophoretic pattern of EthBr stained mixture of supercoiled and relaxed DNA, pDNA (pET29c) after 2 h of electrophoresis. Each sample contained 5 μg of pDNA (0.75 mM in base pairs) incubated with 0.1 and 0.25 mM (upper figure, A) and 0.5 and 1 mM (down figure, B) of each of the compounds at 37 °C for 30 min. **Lane C:** control, plasmid pET29c without treatment. (A), **lanes a and b:** plasmid pET29c treated with 0.1 and 0.25 mM of the compounds **1**, **2**, **3**, **4**, **5** and **6**. (B), **lanes c and d:** plasmid pET29c treated with 0.5 and 1 mM of the compounds **1**, **2**, **3**, **4**, **5** and **6**. Form I represents supercoiled pDNA and Form II represents relaxed pDNA.

supercoil will relax to produce a slower-moving nicked form (Form II, relaxed). If both strands are cleaved, a linear form (Form III, linear) will be generated that migrates in between.[62,63]

The ability of the complexes to effect DNA cleavage has been investigated by gel electrophoresis using supercoiled pET29c DNA in 5 mM Tris-Cl buffer solution pH 7.2. The gel electrophoretic separation of plasmid pET29c DNA products incubated by increasing amounts of the compounds is given in Fig. 9. The results in Fig. 9 indicate that both Form I and Form II of plasmid DNA are slightly up-shifted with the addition of 0.1 and 0.25 mM of the compounds **1**, **2**, **3**, **4**, $[Cu_2(2,4\text{-}D)_4(MeOH)_2]$ (**5**)[64] and $[Cu(2,4,5\text{-}T)_2(MeOH)_2]$ (**6**)[65] (Fig. 9, A). A further increase in the compound concentration causes a much greater up-shift of both Forms (I and II) of plasmid DNA (Fig. 9, B). Especially for the compounds **3** and **4** both Forms (I and II) diminished gradually with a concomitant up-shift, and furthermore they have fully disappeared in the higher concentrations of the compounds 0.5 and 1 mM respectively (Fig. 9, B (lanes 3c, 3d and 4c, 4d), due to the complete DNA degradation suggesting the strong chemical nuclease activity of these compounds comparable to that of enzymic nucleases.

Time-dependence of the pDNA cleavage reaction by {(OH)[9-$MC_{Cu(II)N(PhPyCNO)}$-3]} metallacrowns

The time-dependence of the cleavage reaction of the pET29c DNA, caused by the {(OH)[9-$MC_{Cu(II)N(PhPyCNO)}$-3]} metallacrowns **3** and **4**, was also examined (Fig. 10).

Obviously, the amounts of both forms of the plasmid DNA decreased with time due to a gradual degradation of pDNA, and which almost completed within 30 min ending in its complete disappearance (Fig. 10, lane 3). The obtained pattern is similar for both {(OH)[9-$MC_{Cu(II)N(PhPyCNO)}$-3]} metallacrowns, **3** and **4**. These phenomena imply that these compounds might be characterized as strong chemical nucleases since they induce intensively the cleavage

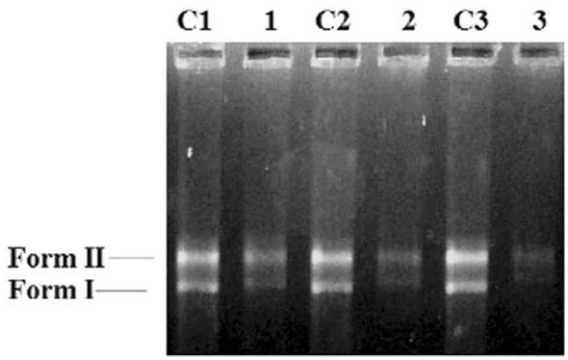

Fig. 10 Time-dependence of the pDNA cleavage reaction by {(μ_3-OH)[9-$MC_{Cu(II)N(PhPyCNO)}$-3]} metallacrowns. Agarose (1% w/v) gel electrophoretic pattern of EthBr stained mixture of supercoiled and relaxed DNA, pDNA (pET29c) after 2 h of electrophoresis. Each sample contained 5 μg of pDNA (0.75 mM in base pairs) incubated with 1 mM of the compound **3** (or **4** respectively) at 37 °C for different incubation times. **Lane C1:** pET29c incubated for 10 min without any compound, **lane 1:** pET29c + compound **3** (or **4**) incubated for 10 min, **lane C2:** pET29c incubated for 20 min without any compound, **lane 2:** pET29c + compound **3** (or **4**) incubated for 20 min, **lane C3:** pET29c incubated for 30 min without any compound, and **lane 3:** pET29c + compound **3** (or **4**) incubated for 30 min. Form I represents supercoiled pDNA and Form II represents relaxed pDNA.

of plasmid pET29c DNA. The cleavage reaction is incubation time-dependent, a fact that may be justified due the prolonged contact of the reaction components.

In order to exclude the occurrence of DNA precipitation, several control reactions have also been carried out to ensure that the trinuclear complexes are responsible for the observed cleavage of pET29c. $Cu(ClO_4)_2$, the ligand phenyl 2-pyridyl ketoxime and the initial materials for the preparation of the trinuclear complexes alone do not show efficient cleavage of pET29c after

30 min, a period during which the {(OH)[9-$MC_{Cu(II)N(PhPyCNO)}$-3]} metallacrowns can cleave pET29c (data not shown). These experiments showed that none of the individual constituents of the complexes (Cu(II), ClO_4^-, or ligands) are responsible for the DNA cleavage but this result is attributed to the integrity (or entity) of the complexes. Besides, DNA precipitation may be excluded from being the cause of DNA disappearance due to the absence of a visible ethidium bromide-stained band in the slots. Similar experiments were performed for the trinuclear copper Cu(II) complexes Cu3–L (L = N,N,N′,N′,N″,N″,-hexakis(2-pyridyl)-1,3,5-tris(aminomethyl)benzene)[24] also confirming this suggestion.

Concentration-dependence of the linearized pDNA cleavage reaction by {(OH)[9-$MC_{Cu(II)N(PhPyCNO)}$-3]} metallacrowns

The effect of concentration-dependence on the interaction reaction of the {(OH)[9-$MC_{Cu(II)N(PhPyCNO)}$-3]} metallacrowns **3** and **4** on DNA that is linearized by the restriction enzyme Hind III pET29c was also examined (Fig. 11).

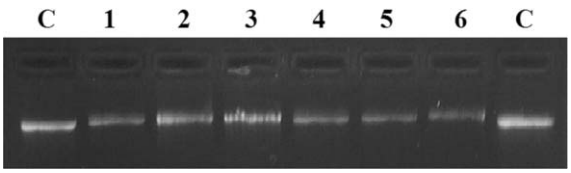

Fig. 11 Agarose (1%w/v) gel electrophoretic pattern of EthBr stained pDNA (pET29c) linearized with the restriction enzyme Hind III. Each sample contained 5 μg of linear DNA incubated with 0.25, 0.5 and 1 mM of the compounds **3** and **4** at 37 °C for 20 min. **Lane C:** control, linearized plasmid pET29c without treatment, **lane 1:** linear DNA + compound **3** (0.25 mM), **lane 2:** linear DNA + compound **3** (0. 5 mM), **lane 3:** linear DNA + compound **3** (1 mM), **lane 4:** linear DNA + compound **4** (0.25 mM), **lane 5:** linear DNA + compound **4** (0. 5 mM), **lane 6:** linear DNA + compound **4** (1 mM).

Gradually increasing the concentration of the {(OH)[9-$MC_{Cu(II)N(PhPyCNO)}$-3]} metallacrowns **3** and **4** resulted in gradual up-shifting of the linearized pDNA which became significantly obvious at a concentration of 1 mM (Fig. 11, lane 3). While an up-shifting of the same order was observed it started even in the presence of the lower concentration (0.25 mM) of compound **4** (Fig. 11, lane 4), increasing only slightly at the higher concentrations tested 0.5 mM (Fig. 11, lane 5) and 1 mM (Fig. 11, lane 6). Moreover, a concomitant decrease of the initial amount of DNA occurred at the higher concentrations due to DNA degradation (Fig. 11, lanes 3 and 6). This experiment clearly shows that these compounds interact with DNA suggesting that a number of {(OH)[9-$MC_{Cu(II)N(PhPyCNO)}$-3]} metallacrown molecules are bound to linear DNA enough to increase its molecular weight and to up-shift such a big molecule reflecting in its delayed electrophoretic mobility and in addition to cause DNA degradation as chemical nucleases.

Mechanistic investigation of the DNA cleavage reaction in the presence of standard radical scavengers

In order to diagnose whether the cleavage mechanism could be attributed to the presence of diffusible radical species and to clarify the oxidative or hydrolytic mode of reaction, we have monitored the quenching of DNA cleavage in the presence of alternative H-donors which would scavenge radicals (such as $^{\bullet}OH$) in solution.[66–69] To this end, standard radical scavengers were added to the reaction of complexes **3** and **4** with DNA. The individual addition of dimethyl sulfoxide (DMSO) (80 mM), ethanol (80 mM) (hydroxyl radical scavenger) and sodium azide (60 mM) (singlet oxygen scavenger) was found to quench DNA cleavage almost completely, compared to that caused by the complexes **3** and **4** without any scavenger (Fig. 12). On adding DMSO or ethanol, the known hydroxyl radical scavengers, the DNA cleavage was almost eliminated indicating that the hydroxyl radicals are involved in the cleavage process. Thus, free radicals participate in the oxidation of the deoxyribose moiety, followed by hydrolytic cleavage of the sugar phosphate backbone in the absence of the scavengers. On the other hand, addition of sodium azide (a singlet oxygen scavenger) decreases the cleavage efficiency strongly revealing that $^1O_2$-derived species might serve as the activated intermediates responsible for the DNA cleavage. These results suggest that in the DNA strand scission reaction caused by these complexes various diffusible oxygen intermediate species (hydroxyl radical or a singlet oxygen) are probably involved.

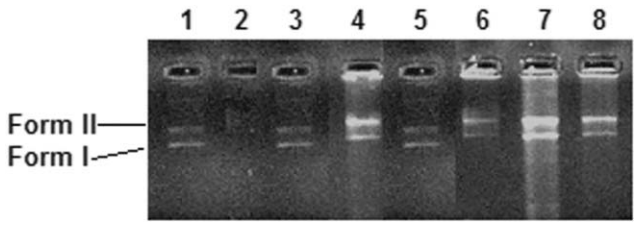

Fig. 12 Agarose (1% w/v) gel electrophoretic pattern of EthBr stained mixture of supercoiled and relaxed DNA, pDNA (pET29c) after 2 h of electrophoresis. Each sample contained 5 μg of pDNA (0.75 mM in base pairs) incubated with 1 mM of compound **3**, with different standard scavengers at 37 °C for 30 min. The obtained pattern is similar for both copper(II) complexes **3** and **4**. **Lane 1:** plasmid pET29c without treatment, **lane 2:** pDNA + compound **3**, **lane 3:** pDNA + DMSO (80 mM), **lane 4:** pDNA + compound **3** + DMSO (80 mM), **lane 5:** pDNA + EtOH (80 mM), **lane 6:** pDNA + compound **3** + EtOH (80 mM), **lane 7:** pDNA + NaN_3 (60 mM), **lane 8:** pDNA + compound **3** + NaN_3 (60 mM). Form I represents supercoiled pDNA and Form II represents relaxed pDNA.

Since these complexes are able to cleave DNA in the absence of any reducing agent we can assume that DNA might be cleaved by a discernible hydrolytic path. The commonly accepted mechanism of hydrolysis of deoxynucleotide phosphates involves nucleophilic attack of a water oxygen on the phosphorus to give a five-coordinate phosphate intermediate.[57,59,70] The present complexes do not contain water in coordination but they have Cu–OH or Cu–OMe groups, which might serve as nucleophilic agents for initiating the DNA attack. However, it has been reported previously that a phosphate–ester bond can be also hydrolytically cleaved by Cu(II) complexes with N-containing ligands[71-74] and this eventuality cannot be ruled out.

Experimental

Safety note

Although no problems were experienced in handling perchlorate compounds, these salts are potentially explosive when combined with

organic ligands and should be manipulated with care and used only in small quantities.

Materials

The chemicals for the synthesis of the compounds were used as purchased. Methanol CH_3OH was distilled over magnesium (Mg) and was stored over 3 Å molecular sieves. EtOH and dimethyl sulfoxide (DMSO) were used without any further purification. $Cu(ClO_4)_2{\cdot}6H_2O$, $CuCl_2{\cdot}2H_2O$, phenyl 2-pyridine ketoxime, 2,4,5-trichlorophenoxyacetic acid and 2,4-dichlorophenoxyacetic acid were purchased from Aldrich Co and used as received. All chemicals and solvents were reagent grade. Agarose was purchased from BRL. Tryptone and yeast extract were purchased from Oxoid (Unipath Ltd., Hampshire, UK). The intercalative dye ethidium bromide (EthBr), guanine, guanosine-5′-monophosphate (GMP) and adenosine-5′-monophosphate (AMP) were purchased from Sigma. Native DNA (dsDNA) (CT-DNA) type I, highly polymerized from calf thymus gland was purchased from Sigma (D-1501). Plasmid DNA, pDNA (pET29c) was isolated from *Escherichia coli* (Top 10) using the GenEluteTM HP endotoxin-free plasmid maxiprep preparation (Sigma-Aldrich), according to the manufacturer's specifications. The pDNA was digested using Hind III restriction endonuclease (Amersham) according to the manufacturer's instructions in order to create linear pDNA.

Instrumentation - physical measurements

Infrared (IR) spectra (400–4000 cm^{-1}) were recorded on a Nicolet FT-IR 6700 spectrometer with samples prepared as KBr pellets. UV–Vis spectra were recorded on a Shimadzu-160A dual beam spectrophotometer. All the fluorescence spectra were recorded by a Hitachi F7000 fluorescence spectrophotometer. The ranges of excitation and emission wavelengths for all the samples were 225–365 and 550–700 nm, respectively. C, H and N elemental analyses were performed on a Perkin Elmer 240B elemental analyzer.

Structure determination

Crystal data and parameters for data collection are reported in Table 6.

The structure was solved by direct methods using the programs SHELXS-97,[75] and refined by full-matrix least-squares techniques on F^2 with SHELXL-97.[76] The phenyl rings of the $PhPyCNO^-$ and 2,4-D ligands were refined with the geometry of the fixed hexagon in order to save parameters and improve the reflections to parameters ratio, but they behave well when left to refine by retaining their geometrical features. All hydrogen atoms were introduced at calculated positions as riding on bonded atoms, except those of the hydroxides which were located in the difference maps and were refined isotropically. All non-H atoms were refined anisotropically, except those of the solvate molecules which were refined isotropically. No H-atoms for the solvate molecules were included in the refinement.

Preparation of the compounds

The preparations of the compounds $[Cu_3(PhPyCNO)_3(\mu_3\text{-}OH)(2,4,5\text{-}T)_2]$ (**2**), $[Cu_3(PhPyCNO)_3(\mu_3\text{-}OCH_3)(Cl)(ClO_4)]$ (**3**) and $[Cu_3(PhPyCNO)_3(\mu_3\text{-}OH)(CH_3OH)_2(ClO_4)_2]$ (**4**) have been reported elsewhere[10,11] while compounds $[Cu_2(2,4\text{-}D)_4(MeOH)_2]$ (**5**) and $[Cu(2,4,5\text{-}T)_2(MeOH)_2]$ (**6**) have been prepared according to the general procedure for $Cu_2(carboxylato)_2(solvent)_2$ complexes.[64,65]

Table 6 Crystal data and structure refinement for $[Cu_3(PhPyCNO)_3(\mu_3\text{-}OH)(2,4\text{-}D)_2]{\cdot}1.25CH_3OH{\cdot}0.25CH_3CN$ (**1**)

	1
Empirical formula	$C_{53.75}H_{43.75}Cl_4Cu_3N_{6.25}O_{11.25}$
Formula weight	1289.62
Temperature	298 K
Crystal system	Triclinic
Space group	$P\bar{1}$
$a =$	14.820(10) Å
$b =$	15.783(8) Å
$c =$	24.900(10) Å
$\alpha =$	90.61(2)°
$\beta =$	94.51(3)°
$\gamma =$	104.34(3)°
Volume	5623(5) $Å^3$
Z	4
Density (calculated)	1.523 Mg m^{-3}
Absorption coefficient	1.379 mm^{-1}
$F(000)$	2620
θ range for data collection	1.42 to 20.65°
Reflections collected/unique	12140/11473 [R(int) = 0.1242]
Reflections used/parameters refined	11473/1292
Index ranges	$-14 \le h \le 0, -15 \le k \le 15, -24 \le l \le 24$
Goodness-of-fit on F^2	1.052
Final R indices [8127 reflections with $I > 2\sigma(I)$]	R_1 =0.0589, wR_2 = 0.1495
Final R indices (all data)	R_1 =0.0929, wR_2 = 0.1756

Preparation of $[Cu_3(PhPyCNO)_3(\mu_3\text{-}OH)(2,4\text{-}D)_2]{\cdot}1.25CH_3OH{\cdot}0.25CH_3CN$ (1). The complex was synthesized by adding 0.9 mmol (0.18 g) of phenyl 2-pyridyl-ketoxime to 0.9 mmol (0.15 g) of $CuCl_2{\cdot}2H_2O$ in 30 mL 10 : 1 methanol–CH_3CN following the addition of 0.6 mmol (0.13 g) of 2,4-DH and 1.8 mmol (0.075 g) of NaOH. The resulting dark green solution was reduced to a volume of 15 mL after 5 h of stirring. The solution was left to slowly evaporate and, in a week, dark green crystals were deposited from the mother liquor. These crystals have been structurally characterized with the formula $C_{53.75}H_{43.75}Cl_4Cu_3N_{6.25}O_{11.25}$ (Fw = 1289.62). Analytical data (Found: C, 50.40; H, 3.30; N, 6.50; requires C, 50.00; H, 3.39; N, 6.78%); Yield 72%. IR: ν_{max}/cm^{-1}: (KBr pellet): $\nu(C{=}N)_{pyridyl}$: 1595(s), ν(N–O): 1460(*vs*), $\nu(CO_2)_{asym}$: 1605(*vs*), 1580(*vs*) $\nu(CO_2)_{sym}$: 1405(s), 1360(s).

Titration spectroscopic studies with DNA and DNA components

DNA binding studies have been performed by UV–Vis spectroscopic titration using buffer A [50 mM Tris((hydroxymethyl)aminomethane)–HCl buffer (pH 7.5)] as solvent. The DNA stock solution (1 mg ml^{-1}, 3×10^3 mM in base pairs) was prepared at 0–4 °C by dissolving the commercially purchased calf thymus DNA in buffer A. DNA concentrations were determined from UV absorption at 260 nm using a molar extinction coefficient of 6600 M^{-1} cm^{-1}. The guanine, GMP and AMP stock solutions (3×10^{-3} M) were prepared by dissolving each of them in buffer A and storing at 0–4 °C. Stock solutions of the complexes were prepared at a final concentration of 2.5×10^{-5} and 5×10^{-4} M by dissolving the complexes in DMSO.

Fluorescence spectroscopic studies

A DNA–EthBr complex was prepared by adding 1.6×10^{-4} M EthBr and 1.6×10^{-4} M DNA in 50 mM Tris–HCl buffer (pH 7.5). The intercalation effect of the complexes with the DNA–EthBr complex was studied by adding a certain volume of the starting solutions of the complexes (3×10^{-3}M) step by step into the solution of the DNA–EthBr complex.

DNA binding/cleavage experiments in agarose gel electrophoresis

The cleavage/binding reaction of DNA with metal complexes was monitored using agarose gel electrophoresis. The DNA cleavage efficiency of the complexes was measured by determining their ability to convert the supercoiled DNA form (SC) to the nicked circular form (NC) and linear form. The DNA binding efficiency of the complexes was estimated by determining the degree of retardation of the mobility reflected in an up-shift of the DNA to higher molecular weight DNA products. Reactions, which contained aliquots of 5 μg of each nucleic acid (0.75 mM in base pairs) (plasmid pET29c or linearized pET29c), were incubated at a constant temperature of 37 °C for 30 min (or as indicated in the legends) in the presence of each compound in a buffer A to a final volume of 20 μl. It was terminated by the addition of 5 μl loading buffer consisting of 0.25% bromophenol blue, 0.25% xylene cyanol FF (acid blue 147) and 30% glycerol in water. The products resulting from interactions of the metal complexes with DNA were separated by electrophoresis on agarose gels (1% w/v), which contained 1 μg ml^{-1} ethidium bromide in 40×10^{-3} M Tris–acetate, pH 7.5, 2×10^{-2} M sodium acetate, 2×10^{-3} M Na_2EDTA, at 5 V cm^{-1}. The standard radical scavengers that were used in the mechanistic investigations of the DNA cleavage reaction were EtOH (80 mM), DMSO (80 mM) and NaN_3 (60 mM). Agarose gel electrophoresis was performed in a horizontal gel apparatus (Mini-SubTM DNA Cell, BioRad) for about 4 h. The gels were visualized after staining with the fluorescence intercalated dye ethidium bromide under a UV illuminator.

Conclusions

In this article, it has been shown that interaction of phenyl 2-pyridyl ketoxime with copper perchlorate in the presence or absence of carboxylato ligands leads to the formation of trinuclear clusters that have been characterized as inverse-9-metallacrown-3 accommodating one or two anions. Interaction of copper inverse {(OH)[9-$MC_{CuN(PhPyCNO)}$-3]} metallacrowns with DNA showed that these compounds bind to dsDNA by intercalative mode leading to hydrolytic cleavage of DNA that may be assigned to the presence of the hydroxyl group in the inverse metallacrown ring. Electrophoretic mobility experiments showed that all complexes, at low cluster concentrations, are capable of binding to pDNA and linear DNA. At higher cluster concentrations and in the absence of any reducing agent they showed markedly chemical nuclease activity. All the complexes behave like chemical nucleases, since they cause the complete degradation of pDNA. Among them, **3** and **4** exhibit the highest nuclease activity, which is abolished in the presence of radical scavengers, indicating that the hydroxyl radicals are involved in the cleavage process.

Acknowledgements

This project is co-funded by the European Union/European Social Fund, "Pythagoras II".

References

1 R. E. P. Winpenny, *Adv. Inorg. Chem.*, 2001, **52**, 1.
2 *Handbook of Metallo-proteins*, ed. A. Messerschmidt, R. Huber, T. Poulos, and K. Wieghardt, John Wiley and Sons, Chichester, UK, 2001.
3 V. L. Pecoraro, A. J. Stemmler, B. R. Gibney, J. J. Bodwin, H. Wang, J. W. Kampf and A. Barwinski, *Prog. Inorg. Chem.*, 1997, **45**, 83–177; J. J. Bodwin, A. D. Cutland, R. G. Malkani and V. L. Pecoraro, *Coord. Chem. Rev.*, 2001, **216–217**, 489–512; G. Mezei, C. M. Zaleski and V. L. Pecoraro, *Chem. Rev.*, 2007, **107**, 4933–5003.
4 C. J. Zaleski, C. Dendrinou-Samara, M. Alexiou, J. W. Kampf, E. Depperman, D. P. Kessissoglou, M. L. Kirk and V. L. Pecoraro, *J. Am. Chem. Soc.*, 2005, **127**, 12862–12872.
5 G. Psomas, A. J. Stemmler, C. Dendrinou-Samara, J. J. Bodwin, M. Schneider, M. Alexiou, J. W. Kampf, D. P. Kessissoglou and V. L. Pecoraro, *Inorg. Chem.*, 2001, **40**, 1562–1570.
6 C. Dendrinou-Samara, L. Alevizopoulou, L. Iordanidis, E. Samaras and D. P. Kessissoglou, *J. Inorg. Biochem.*, 2002, **89**, 89–96.
7 T. C. Stamatatos, J. C. Vlahopoulou, Y. Sanakis, C. P. Raptopoulou, V. Psycharis, A. K. Boudalis and S. P. Perlepes, *Inorg. Chem. Commun.*, 2006, **9**, 814–818; C. J. Milios, A. Vinslava, P. A. Wood, S. Parsons, W. Wernsdorfer, G. Christou, S. P. Perlepes and E. K. Brechin, *J. Am. Chem. Soc.*, 2007, **129**, 8–9; G. C. Vlahopoulou, T. C. Stamatatos, V. Psycharis, S. P. Perlepes and G. Christou, *Dalton Trans.*, 2009, 3646–3649.
8 Th. C. Stamatatos, A. Bell, P. Cooper, A. Terzis, C. P. Raptopoulou, S. L. Heath, R. E. P. Winpenny and S. P. Perlepes, *Inorg. Chem. Commun.*, 2005, **8**, 533–538; Th. C. Stamatatos, E. Diamantopoulou, A. Tasiopoulos, V. Psycharis, R. Vincente, C. P. Raptopoulou, V. Nastopoulos, A. Escuer and S. P. Perlepes, *Inorg. Chim. Acta*, 2006, **359**, 4149–4157; T. C. Stamatatos, E. Diamantopoulou, C. P. Raptopoulou, V. Psycharis, A. Escuer and S. P. Perlepes, *Inorg. Chem.*, 2007, **46**, 2350–2352.
9 T. Afrati, C. M. Zaleski, C. Dendrinou-Samara, G. Mezei, J. W. Kampf, V. L. Pecoraro and D. P. Kessissoglou, *Dalton Trans.*, 2007, 2658–2668.
10 T. Afrati, C. Dendrinou-Samara, C. Raptopoulou, A. Terzis, V. Tangoulis and D. P. Kessissoglou, *Dalton Trans.*, 2007, 5156–5164.
11 T. Afrati, C. Dendrinou-Samara, C. Raptopoulou, A. Terzis, V. Tangoulis, A. Tsipis and D. P. Kessissoglou, *Inorg. Chem.*, 2008, **47**, 7545–7555.
12 N. Kitajima and Y. Morooka, *Chem. Rev.*, 1994, **94**, 737–757.
13 E. I. Solomon, F. Tuczek, D. E. Root and C. A. Brow, *Chem. Rev.*, 1994, **94**, 827–856.
14 Y.-B. Jiang, H.-Z. Kou, R.-J. Wang, A.-L. Cui and J. Ribas, *Inorg. Chem.*, 2005, **44**, 709–715.
15 J. Yoon, L. M. Mirica, T. D. P. Stack and E. I. Solomon, *J. Am. Chem. Soc.*, 2005, **127**, 13680–13693.
16 V. A. Sorokin, V. A. Valeev, G. O. Gladchenko, I. V. Sysa, Y. P. Blagoi and I. V. Volchok, *J. Inorg. Biochem.*, 1996, **63**, 79–98.
17 A. M. Polyanichko, V. V. Andrushchenko, E. V. Chikhirzhina, V. I. Vorob'ev and H. Wieser, *Nucleic Acids Res.*, 2004, **32**, 989–996.
18 B. Lippert, *Prog. Inorg. Chem.*, 2005, **54**, 385–447.
19 A. Sreedhara and J. A. Cowan, *JBIC, J. Biol. Inorg. Chem.*, 2001, **6**, 337–347.
20 J. A. Cowan, *Chem. Rev.*, 1998, **98**, 1067–1088.
21 F. Mancin, P. Scrimin, P. Tecilla and U. Tonellato, *Chem. Commun.*, 2005, 2540–2548.
22 D. R. Graham, L. E. Marshall, K. A. Reich and D. S. Sigman, *J. Am. Chem. Soc.*, 1980, **102**, 5419–5421.
23 S. Goldstein and G. Czapski, *J. Am. Chem. Soc.*, 1986, **108**, 2244–2250.
24 C. Tu, Y. Shao, N. Gan, Q. Xu and Z. Guo, *Inorg. Chem.*, 2004, **43**, 4761–4766.
25 Y. An, S.-D. Liu, S.-Y. Do, L.-N. Ji and Z.-W. Mao, *J. Inorg. Biochem.*, 2006, **100**, 1586–1593.
26 A. Bencini, E. Berni, A. Bianchi, C. Giorgi, B. Valtancoli, D. K. Chand and H.-J. Schneider, *Dalton Trans.*, 2003, 793–800.

27 K. J. Humphreys, K. D. Karlin and S. E. Rokita, *J. Am. Chem. Soc.*, 2001, **123**, 5588–5589.
28 K. J. Humphreys, K. D. Karlin and S. E. Rokita, *J. Am. Chem. Soc.*, 2002, **124**, 6009–6019.
29 K. J. Humphreys, A. E. Johnson, K. D. Karlin and S. E. Rokita, *JBIC, J. Biol. Inorg. Chem.*, 2002, **7**, 835–842.
30 K. J. Humphreys, K. D. Karlin and S. E. Rokita, *J. Am. Chem. Soc.*, 2002, **124**, 8055–8066.
31 J. Chen, X. Wang, Y. Shao, J. Zhu, Y. Zhu, Y. Li, Q. Xu and Z. Guo, *Inorg. Chem.*, 2007, **46**, 3306–3312.
32 J. L. García-Giménez, G. Alzuet, M. González-Álvarez, M. Liu-González, A. Castiñeiras and J. Borrás, *J. Inorg. Biochem.*, 2009, **103**, 243–255.
33 M. González-Álvarez, G. Alzuet, J. Borrás, B. Macías and A. Castiñeiras, *Inorg. Chem.*, 2003, **42**, 2992–2998.
34 Y Zhao, J. Zhu, W. He, Z. Yang, Y. Zhu, Y. Li, J. Zhang and Z. Guo, *Chem.–Eur. J.*, 2006, **12**, 6621–6629.
35 Z. Chen, X. Wangb, Y. Li and Z. Guo, *Inorg. Chem. Commun.*, 2008, **11**, 1392–1396.
36 S. T. Frey, H. H. J. Sun, N. N. Mu-thy and K. D. Karlin, *Inorg. Chim. Acta*, 1996, **242**, 329–338.
37 C. Dendrinou-Samara, G. Tsotsou, C. P. Raptopoulou, A. Kortsaris, D. Kyriakidis and D. P. Kessissoglou, *J. Inorg. Biochem.*, 1998, **71**, 171–179.
38 G. Psomas, C. P. Raptopoulou, L. Iordanidis, C. Dendrinou-Samara, V. Tangoulis and D. P. Kessissoglou, *Inorg. Chem.*, 2000, **39**, 3042–3048.
39 V. Tangoulis, G. Psomas, C. Dendrinou-Samara, C. P. Raptopoulou, A. Terzis and D. P. Kessissoglou, *Inorg. Chem.*, 1996, **35**, 7655–7660.
40 A. Dimitrakopoulou, C. Dendrinou-Samara, A. Pantazaki, C. Raptopoulou, A. Terzis, E. Samaras and D. P. Kessissoglou, *Inorg. Chim. Acta*, 2007, **360**, 546–556.
41 I. Tsivikas, M. Alexiou, A. A. Pantazaki, C. Dendrinou-Samara, D. A. Kyriakidis and D. P. Kessissoglou, *Bioinorg. Chem. Appl.*, 2003, **1**, 85–97.
42 M. Alexiou, I. Tsivikas, C. Dendrinou-Samara, A. Pantazaki, P. Trikalitis, N. Lalioti, D.A. Kyriakidis and D. P. Kessissoglou, *J. Inorg. Biochem.*, 2003, **93**, 256–264.
43 S. A. Tysoe, R. J. Morgan, A. D. Baker and T. C. Strekas, *J. Phys. Chem.*, 1993, **97**, 1707–1711.
44 T. M. Kelly, A. B. Tossi, D. J. McConnell and T. C. Strekas, *Nucleic Acids Res.*, 1985, **13**, 6017–6034.
45 P. Yang, M.-L. Guo and B.-S. Yang, *Chinese Sci. Bull.*, 1994, **39**, 997–1002.
46 E. C. Long and J. K. Barton, *Acc. Chem. Res.*, 1990, **23**, 271–273.
47 J. R. Morrow and W. C. Trogler, *Inorg. Chem.*, 1988, **27**, 3387–3394.
48 E. Kovari, J. Heitker and R. Kramer, *J. Chem. Soc., Chem. Commun.*, 1995, 1205–1206.
49 A. M. Pyle, J. P. Rehmann, R. Meshoyrer, C. V. Kumar, N. J. Turro and J. K. Barton, *J. Am. Chem. Soc.*, 1989, **111**, 3051–3058.
50 K. Mudasir, N. Yoshioka and H. Inoue, *J. Inorg. Biochem.*, 1999, **77**, 239–247.
51 K. Mudasir, K. Wijaya, N. Yoshioka and H. Inoue, *J. Inorg. Biochem.*, 2003, **94**, 263–271.
52 V. Uma, M. Kanthimathi, J. Subramanian and B. Unni Fair, *Biochim. Biophys. Acta, Gen. Subj.*, 2006, **1760**, 814–819.
53 J.-B. LePecq and C. Paoletti, *J. Mol. Biol.*, 1967, **27**, 87–106.
54 Q.-Q. Zhang, F. Zhang, W.-G. Wang and X.-L. Wang, *J. Inorg. Biochem.*, 2006, **100**, 1344–1352.
55 B. C. Baguley and M. Le Bret, *Biochemistry*, 1984, **23**, 937–943.
56 J. R. Lakowicz and G. Weber, *Biochemistry*, 1973, **12**, 4161–4170.
57 B. Selvakumar, V. Rajendiran, P. V. Maheswari, H. Stoeckli-Evans and M. Palaniandavar, *J. Inorg. Biochem.*, 2006, **100**, 316–330.
58 A. Raja, V. Rajendiran, P. U. Maheswari, R. Balamurugan, C. A. Kilner, M. A. Halcrow and M. Palaniandavar, *J. Inorg. Biochem.*, 2005, **99**, 1717–1732.
59 E. L. Hegg and J. N. Burstyn, *Coord. Chem. Rev.*, 1998, **173**, 133–165.
60 J. Liu, T. X. Zhang, T. B. Lu, L. H. Qu, H. Zhou, Q. L. Zhang and L. N. Ji, *J. Inorg. Biochem.*, 2002, **91**, 269–276.
61 R. P. Hertzberg and P. B. Derran, *J. Am. Chem. Soc.*, 1982, **104**, 313–315.
62 D. S. Sigman, *Acc. Chem. Res.*, 1986, **19**, 180–186.
63 A. Sitlani, E. C. Long, A. M. Pyle and J. K. Barton, *J. Am. Chem. Soc.*, 1992, **114**, 2303–2312.
64 G. Smith, E.J. O'Reilly and C. H. L. Kennard, *Inorg. Chim. Acta*, 1981, **49**, 53–61.
65 G. Psomas, C. Dendrinou-Samara, P. Philippakopoulos, V. Tangoulis, C. P. Raptopoulou, E. Samaras and D. P. Kessissoglou, *Inorg. Chim. Acta*, 1998, **272**, 24–32.
66 M. S. Surendra Babu, K. H. Reddy and P. G. Krishna, *Polyhedron*, 2007, **26**, 572–580.
67 F. Wang and L. M. Sayre, *Inorg. Chem.*, 1989, **28**, 169–170.
68 F. Wang and L. M. Sayre, *J. Am. Chem. Soc.*, 1992, **114**, 248–255.
69 Q. Jiang, N. Xiao, P. Shi, Y. Zhu and Z. Guo, *Coord. Chem. Rev.*, 2007, **251**, 1951–1972.
70 M. Komiyama, N. Takeda and H. Shigekawa, *Chem. Commun.*, 1999, 1443–1452.
71 L. A. Basile, A. L. Raphael and J. K. Barton, *J. Am. Chem. Soc.*, 1987, **109**, 7550–7551.
72 J. N. Burstyn and K. A. Deal, *Inorg. Chem.*, 1993, **32**, 3585–3586.
73 J. Chin, *Acc. Chem. Res.*, 1991, **24**, 145–152.
74 N. N. Murthy, M. Mahroof-Tahir and K. D. Karlin, *J. Am. Chem. Soc.*, 1993, **115**, 10404–10405.
75 G. M. Sheldrick, *SHELXS-97, Structure Solving Program*, University of Göttingen, Germany, 1997.
76 G. M. Sheldrick, *SHELXL-97, Crystal Structure Refinement Program*, University of Göttingen, Germany, 1997.